minerals

MDPI

Review

Mineralogy of Zinc and Lead Metallurgical Slags in Terms of Their Impact on the Environment: A Review

Katarzyna Nowińska * and Magdalena Kokowska-Pawłowska

Faculty of Mining, Safety Engineering and Industrial Automation, Silesian University of Technology, ul. Akademicka 2, 44-100 Gliwice, Poland; magdalena.kokowska-pawlowska@polsl.pl
* Correspondence: katarzyna.nowinska@polsl.pl

Abstract: This paper presents the results of a study of the mineralogical and chemical composition of zinc and lead metallurgical slags. These slags contain numerous elements, including toxic metals, which form conglomerates or multiphase intergrowths. The phase composition of slags is one of the main factors that determine their behaviour in weathering environments, that is, their ability to release metals when exposed to atmospheric factors. In this paper, the release of elements from slags and their mobility in a hypergenic environment is determined based on the results of leachability tests and on geochemical modelling, thus assessing the environmental impact of landfilled slags. The elements released from slags in the largest quantities are zinc and lead. Zn is leached out over a long period of time. It was found that after 12 years, the concentration of Zn in the eluate exceeds by 40 times the permissible value of 200 mg/kg for hazardous waste. The degree of leaching of lead from slags as a function of time (after 12 years), despite its significant solubility in water, is much lower than the degree of leaching of zinc. The most mobile phase components of slags in the studied hypergenic environment are the lead phases (anglesite and galena) and, to a lesser extent, the zinc phases (sphalerite and willemite). Anglesite and galena in almost the entire Eh-pH range, along with admixtures of elements, decompose into ionic forms: $PbCl_4^{2-}$, Pb^{2+}, and $PbOH^+$. Sphalerite in the soil and water environment (oxidizing and acidic conditions) will decompose into the mobile ionic form Zn^{2+}. Willemite, which is resistant to weathering, will undergo similar decomposition. It can therefore be assumed that the carriers of toxic metals are primarily lead sulphides and sulphates, zinc sulphides, and, less frequently, zinc, lead, and iron oxides.

Keywords: lead; zinc; slags; metallurgy; mineralogy; environment

Citation: Nowińska, K.; Kokowska-Pawłowska, M. Mineralogy of Zinc and Lead Metallurgical Slags in Terms of Their Impact on the Environment: A Review. *Minerals* **2024**, *14*, 852. https://doi.org/10.3390/min14090852

Academic Editors: Alexandra Guedes, Bruno Valentim and Rui Jorge Coleho de Sousa

Received: 22 July 2024
Revised: 20 August 2024
Accepted: 21 August 2024
Published: 23 August 2024

1. Introduction

Slags resulting from zinc and lead metallurgy are characterised by a diversity of chemical and phase compositions, which in turn depend on the type of feedstock used, the parameters of the technological process applied, and its course [1,2].

These slags contain numerous elements, including toxic metals, i.e., Pb, Zn, Cu, Sn, Sb, Na, Mg, Al, Ca, As, In, Cd, Ag, Au, and Bi, and their phase composition is dominated by complex polyphase conglomerates formed as a result of high-temperature processes [1–5].

Slags from non-ferrous metals metallurgy that are classified as hazardous waste are deposited in landfills and may therefore pose a potential threat to the environment, in particular to soil and water [5].

Determining the adverse environmental impact of landfilled slags requires detailed chemical and mineralogical studies as a basis for predicting the stability of slag constituents under hypergenic conditions [5,6].

The phase composition of slags is one of the main factors determining their stability in weathering environments and their ability to release metals when exposed to atmospheric factors such as precipitation or temperature [5–7].

The most commonly used methods for assessing the degree of environmental mobility of slag minerals are leachability tests conducted under various pH conditions. Less common are methods based on geochemical modelling, hence the application of Eh-pH (Pourbaix) diagrams [8,9], which allow the determination of the regions of stability (within which components occur in mobile soluble forms) and corrosion (within which components occur in insoluble stable forms) for given elemental phases and provide valuable additional information on the forms of occurrence of slag constituents and their behaviour in a hypergenic environment.

2. Zinc and Lead Metallurgical Overview

A total of 20% of the zinc produced globally is obtained using pyrometallurgical methods and 80% is obtained by hydrometallurgical methods [10–12], but most of the studies reviewed here apply to the pyrometallurgical processing of sulphide ores [13,14].

The pyrometallurgical extraction of Zn is dominated by two main processes: the Zn retort process and the Imperial Smelting Process (ISP). The Zn retort process produces Zn metal by reducing ZnO and coke briquettes in a vertical retort furnace or, to a lesser extent, in a horizontal retort furnace. The resulting Zn vapours are collected from the top of the retort and fed to a condenser, where they are cooled and recovered as molten Zn at around 420–450 °C [13–15].

The most widely used pyrometallurgical method for obtaining zinc is the ISP, which is a highly efficient technique that allows for the processing of complex polymetallic raw materials that cannot be processed by other methods.

The ISP is based on the reduction of roasted zinc–lead concentrate with coke [16–18] in a shaft furnace. Lead, liquid slag with a melting point of about 1200 °C, and process gases containing CO_2, CO, N_2, and Zn vapours are formed in the melting zone. Slag and raw lead are periodically discharged from the shaft furnace to the settling tank, from which the slag (shaft furnace slag) is directed to the granulation trough. The raw lead is sent to the refining process. One of the products of this process is refining slag [12–15].

Lead is mainly produced (more than 70% of world Pb production) by the pyrometallurgical processing of sulphide ores. Lead production from ores involves crushing, grinding, and enrichment with flotation, followed by sintering and smelting in a shaft furnace [13,14,19].

3. Methodology for Analysing Zn-Pb Metallurgical Slags

3.1. Chemical and Phase Composition

3.1.1. Elementary Analysis

Methods commonly used to analyse the chemical composition of slags are X-ray fluorescence (XRF)—macro-component analysis—and spectrometric methods (Inductively Coupled Plasma—Mass Spectrometry (ICP-MS), Inductively Coupled Plasma—Atomic Emission Spectrometry (ICP-AES), Inductively Coupled Plasma—Optical Emission Spectrometry (ICP-OES), and Atomic Absorption Spectrometry (AAS))—micro-component (trace element) analysis. X-ray fluorescence relies on the secondary emission of X-rays (fluorescence) from matter that has been excited by high-energy X-ray or gamma-ray bombardment.

Elementary analysis of a sample using interaction with X-rays is carried out by employing one of two measurement techniques [20–22]:

- Energy dispersive spectrometry (EDXRF), in which the measurement of the energy value of the analytical signal and its intensity is carried out using a special detector that counts the number and measures the energy of each photon that reaches it;
- Wavelength dispersive spectrometry (WDXRF), in which the photon stream is dispersed on a suitable crystal that acts as a diffraction grating, and a suitable detector or detector array allows the intensity of the radiation at a specific wavelength to be measured.

The WDXRF method is more sensitive, provides better energy resolution, and covers a wider range of elements (Be to U) compared to the EDXRF method.

Inductively coupled plasma mass spectrometry (ICP-MS) and inductively coupled plasma atomic (optical) emission spectrometry (ICP-AES or ICP-OES) involve decomposed samples in a liquid state that are vaporized using an argon plasma source, during which atoms are converted to ions in the excited state. In the case of ICP-MS, the ions then flow into a mass spectrometer where they are isolated by atomic mass-to-charge ratios using a quadrupole or magnetic sector analyser. A detector then measures the metal ions from the mass spectrometer and calculates their abundance based on signal intensity. In contrast, ICP-AES is based on measuring light emitted from excited atoms and ions instead of a mass measurement [22–24]. ICP-MS and ICP-AES are capable of measuring 70 elements simultaneously with atomic masses ranging from Li to U and sometimes heavier (excluding a few due to interference); ICP-MS has lower levels of detection than ICP-AES [22–24].

Atomic absorption spectrometry AAS is an analytical technique that utilises the phenomenon of the absorption of electromagnetic radiation of a specific wavelength by free atoms in the ground state.

The element to be determined is initially present in the form of a chemical compound from which it must be isolated in the form of free atoms. This is achieved with thermal dissociation in atomisers: a flame atomiser (FAAS) or a graphite-coated furnace (GFAAS). In contrast to the multi-element analysis of ICP-MS and ICP-AES, AAS determines the concentrations of a single particular element. However, both FAAS and GFAAS can be used to determine the concentrations of over 50 different elements.

3.1.2. Phase Analysis and Microanalytical Techniques

To identify the phase composition of slags, the X-ray diffraction (XRD) method is commonly used. It is a non-destructive method, usually with a detection limit of one or more per cent by weight. The principle of the diffractometer is based on the interaction of the X-ray beam with the crystal structure of the sample. The radiation source is usually a Co, Cu, or Mo tube. Some of the scattered X-rays undergo constructive interference or diffraction and allow for the identification of the structure of a mineral based on Bragg's law. Crystalline mineral phases as well as amorphous phases, including glass, can be quantified using techniques such as Rietveld analysis and diffraction profile fitting [25].

One of the most commonly employed microanalytical techniques is electron probe microanalysis (EPMA), which is used to analyse the chemical composition of crystalline phase grains within a micro-area. X-ray electron microanalysis utilises the interaction of high-energy electrons of the beam with the electrons of the inner shells of the atoms of which the sample under examination is composed. Registering the characteristic X-rays emitted by the excited electrons provides information on the chemical composition of the sample under examination, while registering elementary particles, i.e., secondary and backscattered electrons, allows the surface of the mineral under examination to be imaged. The characteristic X-rays are detected at particular wavelengths, and their intensities are measured to determine concentrations. This analytical technique has a high spatial resolution and sensitivity, and individual analyses are reasonably short, requiring only a minute or two in most cases. Additionally, the electron microprobe can function like a scanning electron microscope (SEM) and provide highly magnified secondary- and backscattered-electron images of a sample [6,26].

Characteristic X-rays can be detected using two methods: energy dispersive spectroscopy EDS and wavelength dispersive spectroscopy WDS. These two methods complement each other, as the wavelength and energy of the characteristic X-rays are interrelated.

In the EDS method, the energy spectrum distribution of the characteristic X-rays is measured. Typically, the active element of an EDS detector is made of a Si(Li) semiconductor. During the measurement, the entire spectrum of emitted X-rays is recorded. This method allows compositional analysis from a selected area, point-wise and profile-wise along a designated line, and the mapping of the distribution of individual elements on the sample surface. The EDS method is used in both scanning and transmission electron microscopy [21,26].

The WDS method, on the other hand, utilises X-ray diffraction on an analysing crystal, following Bragg's law. The deflected X-rays are recorded by a detector (usually a proportional gas counter) [21,27].

While EDS yields more information and typically requires a much shorter counting time, WDS is generally more precise with lower limits of detection due to its superior X-ray peak resolution and greater peak-to-background ratio.

In addition to electron microprobe analysis (EMPA), scanning electron microscopy (SEM) is also commonly used to characterise slags. It enables the imaging of the structures and morphology of the materials under analysis by means of a focused electron beam, scanning line-by-line sections of the surface of the samples under examination. Analogue-to-digital processing of the signals, which are recorded with detector systems as a result of the interaction of the emitted electrons with the material under examination, results in a two-dimensional image or X-ray spectrum [21,26,28].

Scanning electron microscopes offer the ability to take images of the examined materials at magnifications of up to 300,000 times in three basic modes of operation: low voltage, high vacuum (HV), and low vacuum (LV). In particular, the use of the low vacuum (LV) mode allows delicate, vulnerable objects to be imaged, thus making it possible to skip the preparation step that is typical with non-conducting materials. In addition, SEM microscopes are fitted with X-ray microanalysis systems for qualitative and quantitative measurements of the chemical composition of samples with energy dispersion EDS or wavelength dispersion WDS [21,26,27].

3.2. Leachability Tests

The environmental impact of slags is determined based on the results of leachability tests (dynamic and static), simulating natural slag weathering processes or landfill conditions. These tests help determine the mobility of elements contained in slags and predict their long-term (up to several hundred years) behaviour in the environment [1,2,29,30].

There are many types of leach test procedures that vary based on the sample preparation, leachant composition, method of contact, solid-to-solution ratio, leachant renewal, temperature, contact time, and, ultimately, purpose, among others. The most commonly employed leaching tests can be divided into several types. One method, the single batch test, developed by the United States Environmental Protection Agency (USEPA) for regulatory compliance includes a leaching procedure with toxicity characterisation (Toxicity Characteristic Leaching Procedure—TCLP) [1,2,29,30]. This procedure replaced the extraction procedure toxicity test (EP-tox) and the synthetic precipitation leaching procedure (SPLP) (USEPA, 2008). Another single batch test procedure is that described in the EN 12457-2 standard [31] introduced by the European Committee for Standardisation (European Committee for Standardisation, 2002) (Figure 1).

There are also other methods used for static leaching of components. Based on the American standard ASTM-D5284 (2009) [32], according to which contaminant leachability tests are conducted using static acid tests with different dry solids to leachant ratios (depending on the characterised natural conditions of waste storage), a test is conducted in which the leachant is a weakly acidic solution (pH 5.5) and the dry solids to solution ratio is 1:10. Such conditions allow the effect of pH on the rate of leaching of constituents (heavy metals) from the waste to be determined, and thus on the rate of generation of constituents migrating into the soil and water environment under natural conditions (being similar to the natural pH of the environment and the precipitation water leaching the waste).

The extraction solutions used for the elemental leachability tests conducted on Zn-Pb metallurgical slags were organic acids and hyperalkaline buffer solutions. These tests were mostly carried out for elements with an average content in slags of more than several per cent, i.e., Zn, Pb, Fe, Cu, Cd, and As [1–3,29,30,33].

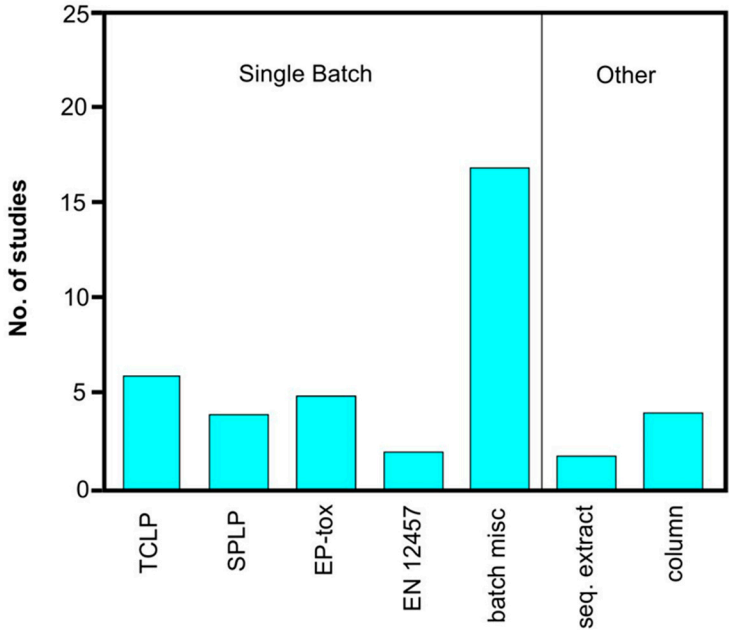

Figure 1. Methods used for leaching tests based on [4].

The leaching degree of individual elements from slags is calculated using the formula for the standardised Qn factor [4]:

$$Q_n = \left[\frac{[E_1]}{AW} * \left(\frac{V}{W}\right) * \left(\frac{1}{SA}\right)\right]_{eluate} / \left[\frac{[E_2]}{AW} * \left(\frac{1}{SA}\right)\right]_{slag} \quad (1)$$

where: Qn—normalised element concentration [mole $\times$ m^{-2}], $[E_1]$—element content in the eluate [ppm], $[E_2]$—element content in the slag [ppm], V—volume of the eluate [mL], AW—standard atomic weight of the element, W—slag weight [g], and SA—specific surface area of slags [$m^2 \times g^{-1}$]. Taking into account the leaching time t [days], leaching curves are determined using the following formula:

$$\log\ R_e = \log\left[\frac{[E_1]}{AW} * \left(\frac{V}{W}\right) * \left(\frac{1}{SA * t}\right)\right]_{eluate} \quad (2)$$

3.3. Geochemical Modelling

The results of the leachability tests carried out are most often complemented by geochemical modelling. For more than 20 years, many researchers have used elemental speciation modelling to study the reactivity of landfilled wastes (including slags) in a hypergenic environment. Geochemical modelling is also the basis for identifying secondary minerals that crystallise in the slags as a result of environmental factors [4,33,34].

The reliability of modelling results is often limited by the incomplete mineralogical characterisation of the slags, insufficient data on the environmental conditions of the study area, and a lack of thermodynamic parameters of the mineral phases and their aqueous solutions. In order to improve the quality of the geochemical models obtained, it is essential to take into account the solubility kinetic coefficients of both the mineral phases and glass present in the slags. Due to the varying chemical composition of the glass, taking these coefficients into account is problematic [35,36].

One of the most commonly used modelling methods is that which uses PHREEQC—a computer program for speciation, batch-reaction, one-dimensional transport, and inverse geochemical calculations. There are a number of other software tools for geochemical modelling based on thermodynamic equilibrium models, e.g., MINTEQA2, Visual MINTEQ, EQ3NR, or CHESS/HYTEC. Advanced modelling approaches, such as reaction path modelling (code EQ62) and kinetic modelling (code KINDIS(P)63), require the input of calcu-

lated/estimated dissolution rate constants, which for most primary slag phases (e.g., glass) are not available [35–38].

Another of the geochemical modelling methods is based on Eh and pH diagrams using HSC Chemistry software version 9. The diagrams were plotted for conditions characteristic of the soil and water environment of the landfill area where the slags are deposited.

Studies are performed within the water stability region, within the Eh range of −0.6…+1.2 V and a pH consistent with that of the soil and water environment of the site. From the average percentages of the individual main phases and their solubilities in the soil and water environment, the concentrations of the components taken for modelling are calculated. The concentrations of trace dopant elements in the main phases are determined as proportional averages of their concentration in a phase to the solubility of that phase (at a set temperature) [5,39].

4. Chemical and Mineral Composition of Slags from Zn-Pb Metallurgy

4.1. Chemical Composition

Slags from Zn-Pb metallurgy contain a number of chemical constituents, of which the dominant ones are the following: SiO_2, Al_2O_3, FeO_{Total}, MgO, CaO, CuO, ZnO, and PbO [1–5,13,14] (Table 1).

Table 1. Summary of major chemistry (in wt%) and minor chemistry (in mg kg^{-1}) of Zn-Pb metallurgical slags and Pb refining slags [1,5].

Component	Zn-Pb Slags			Pb Refining Slags		
	Min	**Max**	**Average ***	**Min**	**Max**	**Average ****
SiO_2	2.04	57.1	28.6	2.45	35.5	11.1
Al_2O_3	0.90	21.9	8.3	0.57	7.8	2.8
FeO_{Total}	0.88	59.6	16.7	8.3	31.1	20.0
MgO	0.61	15.9	5.4	0.10	0.81	1.1
CaO	0.18	32.2	17.3	0.14	5.65	2.8
CuO	0.0020	0.93	0.10	0.98	20.93	11.5
SO_3	0.05	14.9	2.99	5.83	23.1	13.6
MnO	0.01	3.0	0.50	0.02	0.55	0.21
K_2O	0.02	3.91	0.60	0.04	0.27	0.15
ZnO	0.03	47.2	4.93	6.6	18.07	12.2
PbO	0.0002	6.4	0.93	0.72	44.6	17.8
TiO_2	0.07	1.14	0.40	0.04	0.34	0.16
Element	Min	Max	Average	Min	Max	Average
Ba	76	17,914	1126	336	778	508
Ni	13	240	60	76	447	311
Co	8.5	242	36	0.01	452	232
Cr	4.0	700	155	132	708	435
As	1.0	10,710	1181	147	15,558	8843
Cd	0.38	575	31	85	19,757	5595
Sb	0.16	245	43	81	9869	472
Sn	0.10	500	23	0.01	617	323

*—arithmetic average values according to [1], **—arithmetic average values of samples according to [5].

Refining slags show a different chemical composition from that of slags from the shaft process of Zn-Pb metallurgy, as they are dominated by ZnO (average content 12.2 wt%), PbO (average content 17.5 wt%), CuO (average content 11.5 wt%), and SO_3 (average content 13.6 wt%), while in slags from the shaft process their average content is several times lower (Table 1). In addition to the main constituents represented in oxide form, Zn-Pb metallurgical slags contain numerous minor constituents, including the following: Ba, Ni, Co, Cr, As, Cd, Sb, and Sn, the concentrations of which also vary over a wide range (Table 1).

4.2. Mineral Composition

The phase composition of Zn-Pb metallurgical slags varies widely, with the main phase components of slags being as follows [1–5,40–60] (Figures 2 and 3):

- Oxides and hydroxides: zincite ZnO, wüstite FeO, hematite Fe_2O_3, and goethite FeO(OH);
- Sulphides: sphalerite ZnS, galena PbS, pyrite FeS_2, pyrrhotite FeS, digenite $(Cu,Fe)_9S_5$, cubanite $CuFe_2S_3$, covellite CuS, and chalcocite Cu_2S;
- Sulphates and hydrated sulphates: anglesite $PbSO_4$, goslarite $ZnSO_4{\cdot}7H_2O$, gypsum $CaSO_4{\cdot}2H_2O$,rapidcreekite $Ca_2(SO_4)(CO_3){\cdot}4H_2O$, ktenasite $ZnCu_4(SO_4)_2(OH)_6{\cdot}6H_2O$, posnjakite $Cu_4[(OH)_6 \mid SO_4]{\cdot}H_2O$, and namuwite $Zn_4(SO_4)(OH)_6 \cdot 4H_2O$;
- Silicates and aluminosilicates: willemite Zn_2SiO_4, olivines (Mg, Fe, Mn)SiO_4, including fayalite Fe_2SiO_4, kirschsteinite $CaFe_2 + SiO_4$ and forsterite Mg_2SiO_4, pyroxenes, and melilites $(Ca,Na)_2(Al,Mg)[(Si,Al)_2O_7]$, which usually form complex conglomerates or multiphase intergrowths;
- Carbonates: cerussite $PbCO_3$, smithsonite $ZnCO_3$, hydrozincite $Zn_5[(OH)_3/CO_3]_2$, hydrocerussite $Pb_3(CO_3)_2(OH)$, and calcite $CaCO_3$;
- Nitrates: gerhardite $Cu_2(NO_3)(OH)_3$;
- Spinels, mainly magnetite. Further on: hercynite $FeAl_2O_4$, franklinite $ZnFe_2O_4$, gahnite $ZnAl_2O_4$, and ulvite Fe_2TiO_4;
- Metal alloys (Pb, Zn, Cu, Fe, As, Sb) and pure metals (Zn, Pb, Cu, Fe).

The mineral composition of Zn-Pb slags is determined by their chemical composition and crystallization conditions (temperature, cooling rate).

For example, olivine-group phases are very common in crystalline slags; therefore, fayalite (Fe_2SiO_4), kirschsteinite ($CaFeSiO_4$), and forsterite (Mg_2SiO_4) were found to be dominant in many Pb–Zn slags. Melilite-group phases crystallize mostly from the Ca-rich slag melts [1,5].

In the Zn-Pb metallurgical slags, in addition to the crystalline components, there is an amorphous substance—glass, the amount of which depends on the cooling rate of the slags. Glass content in slags quickly cooled with water is much greater than in slags cooled slowly, e.g., in an air atmosphere [60–63].

Rapidly quenched slags (e.g., granulated) have very simple phase compositions with dominant glass, while air-cooled slags are characterized by much more complex mineral compositions, but the formation of phases generally starts with the formation of the crystalline components and ends with the solidification of glass.

The difficulty in quantifying glass is due to its amorphous nature and the varying silica SiO_2 content resulting in an ambiguous interpretation of the reflections related to the corresponding d_{hkl} interplanar spacing values in X-ray structural studies [6,63].

Glass also contains elements such as the following: Fe, Al, Ca, Pb, Zn, Cu, and As, which occur in the form of nanometric oxide inclusions and intermetallic compounds [6].

In the phase composition of slags, in terms of genesis, the following components are distinguished:

- Originating from the technological process (mainly silicates and aluminosilicates; sulphate: anglesite; oxides: wüstite, zincite);
- Crystallizing in hypergenic conditions in the landfill (mainly sulphates and hydrated sulphates: ktenasite, namuwite, posnjakite; hydroxide: goethite; nitrate: gerhardite; carbonates: cerussite, calcite);
- Having the character of source minerals (mainly ZnS and PbS sulphides).

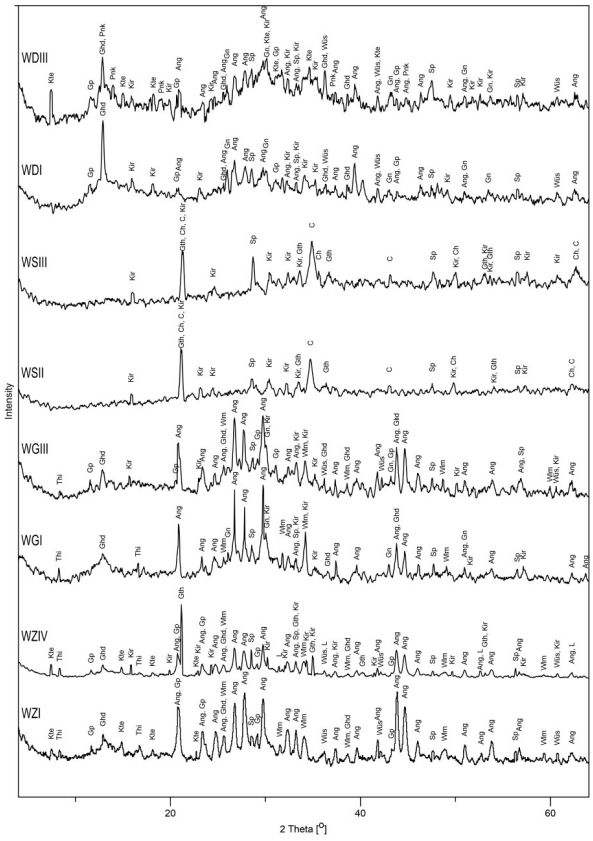

Figure 2. Examples of diffractograms of Zn-Pb slag samples (WDIII, WDI, WSIII, WSII, WGIII, WGI, WZIV, WZI) [36]. Explanations: Ang—anglesite, C—carnegieite, Ch—$Na_2Zn(Si_2O_6)$, Gp—gypsum, Gn—galena, Ghd—gerhardite, Gth—goethite, Kir—kirschteinite, Kte—ktenasite, Ol—oliwin, L—metallic lead, Pnk—posnjakite, Nmw—namuwite, Sp—sphalerite, Thi—tochilinite, Wlm—willemite, Wüs—wüstite (abbreviations of mineral names according to [64]).

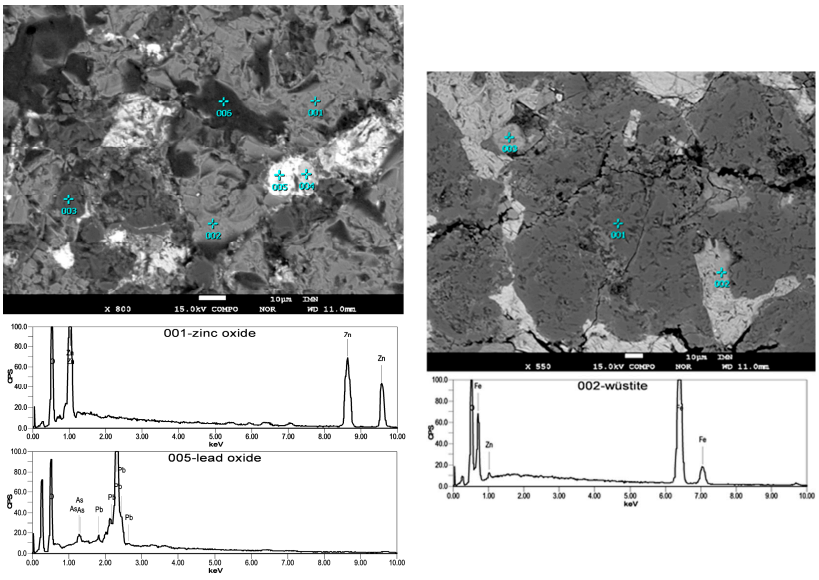

(**a**) (**b**)

Figure 3. Example of an image with examples of EDS spectra of the investigated micro-areas of Zn-Pb samples. (**a**) 001 and 002-wüstite and zinc oxide in glass, 003-willemite, 004-alamosite, 005-lead oxide, 006-quartz, (**b**) 001, 002-kirschteinite with $Na_2Zn(Si_2O_6)$ and carnegieite with admixtures of sphalerite, 003-Ag met [5].

5. Environmental Aspects

5.1. Slag Leaching Properties

Constituents released from slags during weathering and reactions with the surface and groundwater can have an adverse effect on the environment. The behaviour of slags during leachability tests is strongly dependent on their chemical and phase composition.

Studies carried out by a number of authors have shown a significant degree of elemental leaching from metallurgical slags deposited in landfills located in Příbram, Czech Republic; New Brunswick, Canada; Upper Silesia, Poland; São Domingos mining district, and Portugal; Illinois, USA, with some of the elements subsequently being bound in secondary minerals formed under hypergenic environmental conditions, which significantly reduced their mobility [65–70]. As mentioned, one of the factors determining the solubility of the components present in slag and their mobility in the environment is their mineralogical and chemical composition. Silicate and spinel phases were found to be the most resistant to weathering processes, while sulphide, glass, and intermetallic phases [66–68] showed much higher solubility in the soil and water environment.

The elements released from slags in the greatest quantity and characterised by significant solubility of more than 2.0 mg/L include zinc, lead, and iron. Zn leaching occurs over a long period of time, and it was found that after 12 years the Zn concentration in the eluate exceeded the 200 mg/kg limit for hazardous waste by 40 times [6,34,36,45,57,67] (Figure 4). Under the pH conditions (4.5–6.0) of a hypergenic environment, zinc occurs mainly in the form of Zn^{2+} and $ZnCO_3^{+}$, rarely $ZnSO_4 \cdot 7H_2O$. Zinc mobility in near-neutral environments is limited as the element is readily adsorbed by oxides, hydroxides, and aluminosilicates [4,35,38,40,49,67].

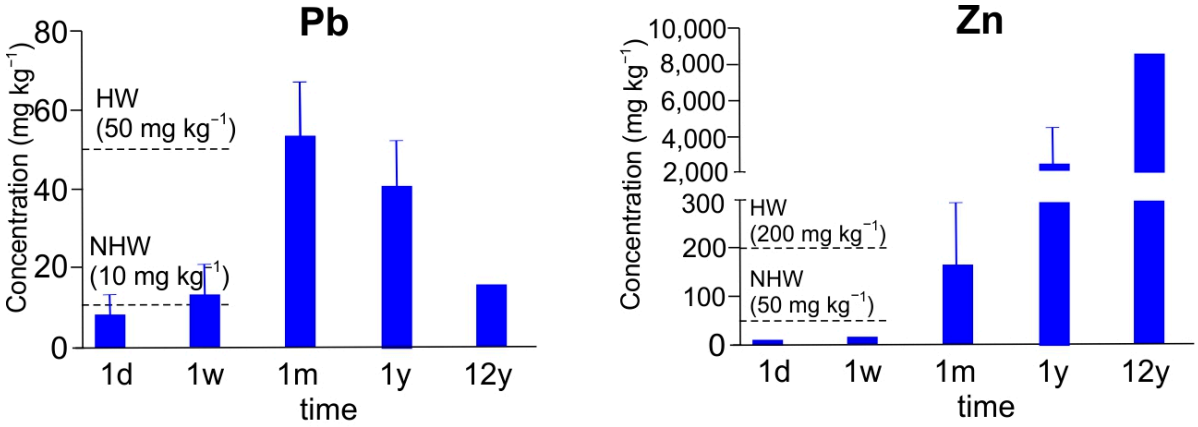

Figure 4. Example of the leaching of Pb and Zn from Pb smelting slags. Explanation: NHW—the EU limit values for non-hazardous waste, HW—the EU limit values for hazardous waste, based on [6].

In the case of the release of zinc into the environment, a high zinc content in the soil negatively affects its properties. With a zinc content above 100 ppm, nitrification processes are limited in the soil, and if its amounts exceed 1000 ppm, it negatively affects most microbiological processes [5].

The leaching degree of lead from Zn-Pb metallurgical slags as a function of time (after 12 years), despite its considerable solubility in water (>2 mg/L), is significantly lower than that of zinc.

This is due to the fact that the release of Pb is partly limited by the formation of new phases, such as the following: lead carbonates and sulphates (e.g., cerusite $PbCO_3$ and angositite $PbSO_4$), which are insoluble in water. Increased lead mobility is significantly influenced by the salinity of the subsurface zone waters, which promotes the formation of soluble $PbCl_2$, $PbCl_4^{-2}$ and $PbCl^{+}$ complexes [4,38,65–67,71–74].

Lead is a highly toxic metal, so when released into the environment it poses a threat to both fauna and flora. Lead and its inorganic compounds, according to the International

Agency for Research on Cancer (IARC—International Agency for Research on Cancer), are classified in group 2B, i.e., substances possibly carcinogenic to humans [5]. The most common is chronic poisoning with Pb and its compounds, called lead poisoning, manifesting itself primarily in neurological and mental disorders. Excess lead in plants disrupts the photosynthesis process.

Environmental pH is one of the key parameters affecting the dissolution of the mineral phases of Zn-Pb slags, thus affecting the release of elements and their stability in the environment [4,67–69,71,72].

The pH-dependent leaching trends of selected contaminants (As, Cu, Pb, and Zn) eluted from metallurgical slags are shown in Figure 5. Interestingly, despite considerable variability in chemical and mineral composition, the leaching curves show marked trends [1,72–76].

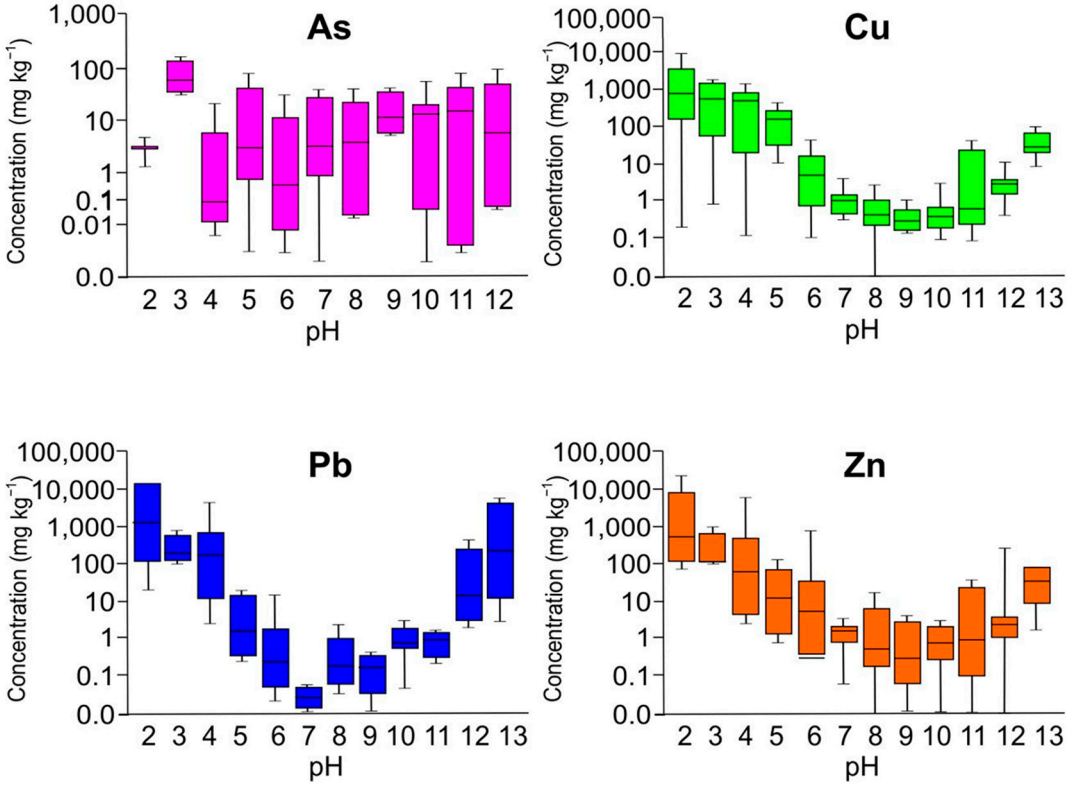

Figure 5. Dependence on pH of leaching of main elements from non-ferrous metal slags, based on [1,6,72–74,77–79].

The leaching of arsenic (which occurs in the leachate mainly as oxyanionic species, such as $H_2AsO_4^-$, $HAsO_4^{2-}$, and AsO_4^{3-}) is relatively flat with slightly higher medians of leaching at a low pH and under alkaline/highly alkaline conditions (medians up to 62 mg·kg^{-1} and up to 16 mg·kg^{-1}, respectively (Figure 5)) [1,6,72–74,77,78].

Arsenic in the +3 oxidation state is more toxic than in the +5 oxidation state [5]. This element is highly toxic to living organisms, and according to IARC it is classified in the first group of carcinogenic substances, which includes compounds with epidemiologically proven carcinogenic effects [5].

Copper and zinc exhibit mainly cationic behaviour with the highest leaching under strongly acidic conditions (Cu: median 921 mg·kg^{-1}; Zn: median 494 mg·kg^{-1} at pH = 2), with the lowest leaching under slightly alkaline conditions (ca. 3–4 orders of magnitude lower than at pH = 2) (Figure 5) [1,6,72–74,77,78].

Lead shows properties typical of amphoteric compounds, with the highest level of leaching under strongly alkaline and strongly acidic conditions and the lowest level of

leaching under neutral conditions pH = 7 (up to 5 orders of magnitude difference between extreme and neutral pH values) (Figure 5) [1,6,71–74,77–81].

5.2. Mobility of Metals and Metalloids from Zn-Pb Slags in Soil and Water Environment Based on Geochemical Modelling

Due to the complexity of the mineral composition of the metallurgical wastes studied, in which multiphase conglomerates predominate, it is difficult to determine unambiguously the environmental mobility of the constituent elements [71,79,80].

Based on the geochemical modelling performed by the authors [6,34–39] using PHREEQC and HSC Chemistry software, the stability in a hypergenic environment of the main components of Zn-Pb slags was determined, taking into account the admixtures contained therein.

Figure 6A shows the key Pb-bearing phases that control the pH-dependent release of lead into the environment based on PHREEQC; Figure 6B shows the phase distribution of chromium as a function of environmental pH values resulting from geochemical modelling using LeachXS™ software 3.0.0. [6].

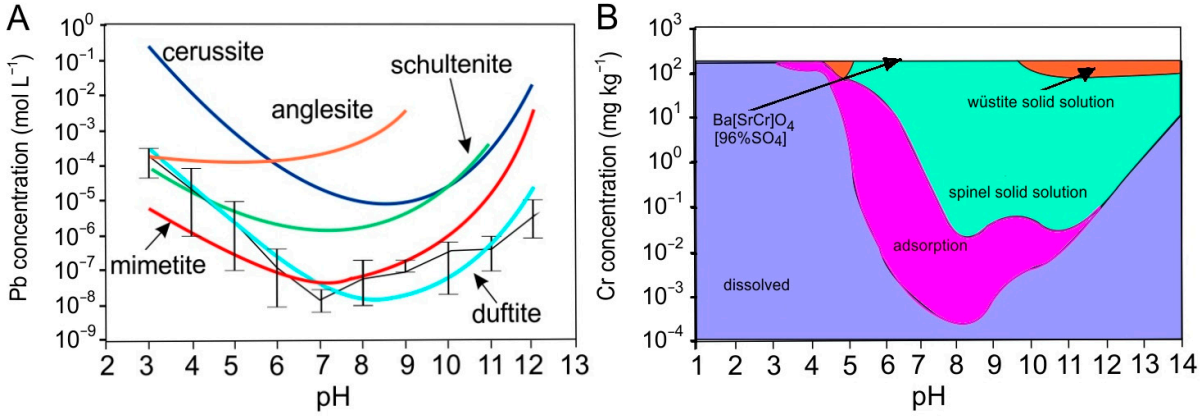

Figure 6. Geochemical modelling: (**A**) dependence of Pb solubility on pH based on PHREEQC; (**B**) the phase distribution of chromium as a function of environmental pH values based on LeachXS™ software. Data compiled and redrawn from [6].

Table 2 shows a summary of the forms in which the elements released from the main phases of Zn-Pb slags occur based on HSC Chemistry modelling. The following values of environmental parameters were assumed in the modelling: average precipitation—700 mm/year and average annual temperature +17 °C. The calculations were carried out within the water durability field for the following range of pH values: 4÷8, consistent with conditions of the soil and water environment in the research area.

The most mobile of the analysed slag constituents in the hypergenic environment studied is anglesite, which decomposes and forms mainly the ionic forms $PbCl_4^{2-}$, Pb^{2+}, and $PbOH^+$, the exceptions being the stable molecular forms PbS under reducing conditions and PbO_2 under a narrow range of oxidising conditions in an alkaline environment (Table 2, Figure 7) according to the following reactions [81–85]:

$$Pb^{+2} + SO_4^{-2} \rightleftharpoons PbSO_4 \quad (3)$$

$$4Cl^- + Pb^{+2} \rightleftharpoons PbCl_4^{-2} \quad (4)$$

$$Pb^{+2} + H_2O \rightleftharpoons PbOH^+ + H^+ \quad (5)$$

$$Pb^{+2} + HS^- \rightleftharpoons PbS + H^+ \quad (6)$$

$$Pb^{+2} + 0.5O_2 + H_2O \rightleftharpoons PbO_2 + 2H^+ \quad (7)$$

Table 2. Forms of occurrence of main elements Pb and Zn released from the main phases of Zn-Pb slags into groundwater environment [5].

Main Phase in Zn-Pb Slag	Form of Occurrence		
	Environment (pH Value)	Reducing Conditions	Oxidizing Conditions
$PbSO_4$	acidic	PbS, Cd^{2+}	$PbCl_4^{2-}$, Pb^{2+}
	neutral	PbS, Cd^{2+}	$PbCl_4^{2-}$, $PbOH^+$
	alkaline	PbS, $PbOH^+$	$PbCl_4^{2-}$, $PbOH^+$, PbO_2
PbS	acidic	Pb^{2+}, PbS,	$PbCl_4^{2-}$, Pb^{2+}, PbS
	neutral	$PbCO_3$, PbS	$PbCl_4^{2-}$, PbS
	alkaline	PbS, $PbCO_3$	$PbCl_4^{2-}$, PbO_2
ZnS	acidic	ZnS	Zn^{2+}
	neutral	ZnS	Zn^{2+}
	alkaline	ZnS	$Zn_5(OH)_6(CO_3)_2$
Zn_2SiO_4	acidic	Zn^{2+}	Zn^{2+}
	neutral	Zn^{2+}	Zn^{2+}
	alkaline	Zn^{2+}	Zn^{2+}

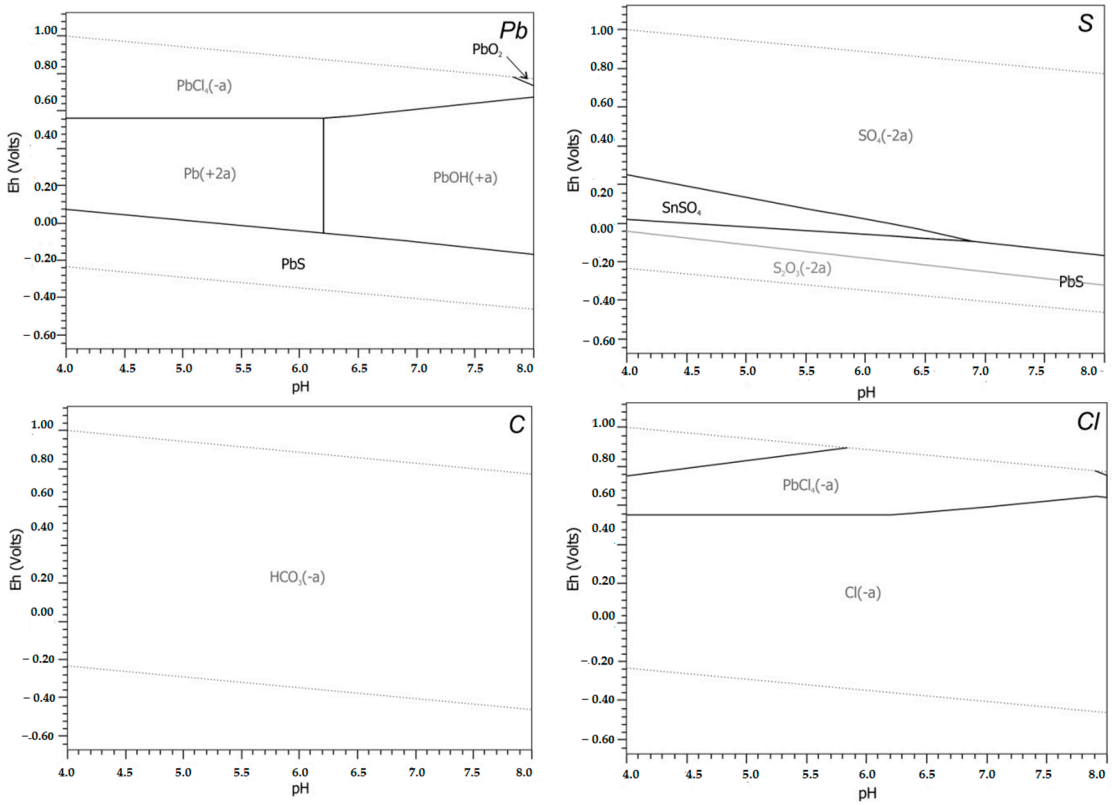

Figure 7. Sample Eh-pH diagrams for $PbSO_4$, taking into account the presence of CO_2 and Cl^- ions in the environment (temperature T = 17 °C) [5].

These findings are corroborated by studies by other authors [4,5,8,9,61,71,79].

Arsenic, which is released into the environment with the anglesite, occurs throughout the Eh-pH range in ionic forms, with the less toxic ions predominating, where the oxidation state of As is +5 [5,39].

Cadmium, over almost the entire Eh-pH range, occurs in Cd^{2+} ionic forms, except for a narrow range in acidic environment (pH < 7.0) under oxidising conditions (Eh > 0.40), where it forms the stable molecular form $Cd(OH)_2$ [5,39].

Cadmium is a highly toxic element that enters the environment in its ionic form. Cd, among others, negatively affects the metabolism of other elements, such as zinc, copper, magnesium, iron, and others, changing the morphology and functions of specific organs. For example, by replacing zinc in biological reactions, it disrupts the synthesis of DNA, RNA, and proteins, as well as the enzymatic activity of enzymes containing Zn [5].

Tin that is present in anglesite, in the hypergenic environment studied, occurs both in mobile ionic forms characteristic of strongly acidic (pH < 5.0) and slightly basic (pH > 6.5) environments and in stable molecular forms characteristic of acidic environments (pH = 5.0. . .6.5), except for reducing conditions in the range Eh = 0.00. . .0.20 V. Sb released with $PbSO_4$ into the environment is stable in the environment, and its exclusive forms of occurrence are oxides [39,83].

The dissolution of anglesite may result in the formation of acidic wastewater that affects the chemistry of surface waters or infiltrates into soils, causing their acidification and thus increasing the mobility of the pollutants contained in them [5].

The PbS present in the slags decomposes in the environment studied, forming both mobile (ionic) and stable (molecular) forms of lead. The ionic forms Pb^{2+} are characteristic of oxidising and weakly reducing conditions in acidic environments (pH < 5.8), while $PbCl_4^{2-}$ is characteristic of strongly oxidising conditions (Table 2, Figure 8).

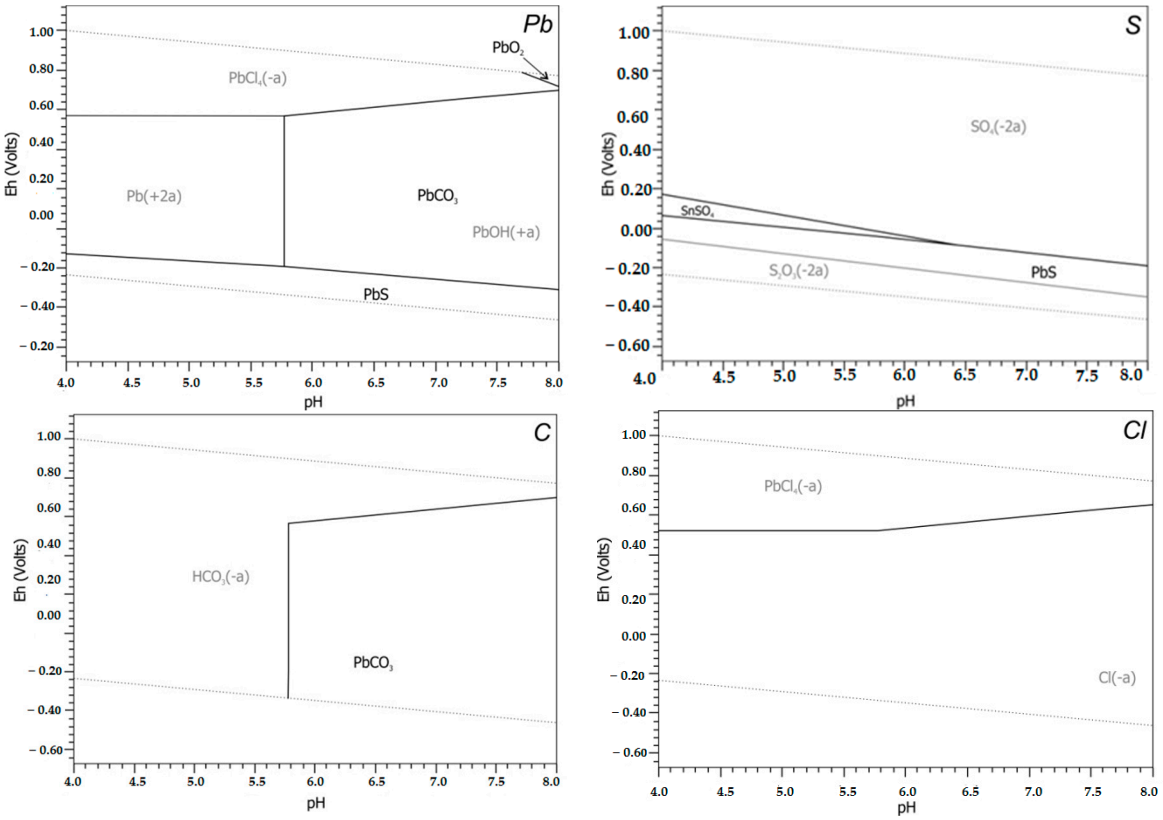

Figure 8. Sample Eh-pH diagrams for PbS, taking into account the presence of CO_2 and Cl^- ions in the environment (temperature T = 17 °C) [5].

Stable $PbCO_3$, co-occurring with the $PbOH^+$ ion (Equation (9)), is the predominant form of Pb in environments with pH > 5.8, while PbS and PbO_2, as in the case of anglesite, occur under reducing conditions and in alkaline environments under oxidising conditions, respectively [37,85–88]:

$$HCO_3^- + Pb^{+2} \rightleftharpoons PbCO_3 + H^+ \quad (8)$$

$$Pb^{+2} + H_2O \rightleftharpoons PbOH^+ + H^+ \quad (9)$$

Cadmium, released into the environment with galena, is present only in mobile ionic form, while in the case of tin, a reduction in the $Sn(OH)_4$ and $SnSO_4$ stability regions can be observed compared to Eh-pH diagrams compiled for $PbSO_4$ [5,39,83].

Antimony released into the environment with PbS, as is the case with $PbSO_4$, is stable in the environment, and its exclusive forms of occurrence are oxides.

Sphalerite, upon entering the environment under study from slags deposited in the landfill, is decomposed, and the predominant form of zinc in the oxidising conditions of this environment for pH < 7.2 is the mobile Zn^{2+} ion (Equation (10)), and the stable forms are as follows: ZnS characteristic for reducing conditions and $Zn_5(OH)_6(CO_3)_2$ (Equation (11)) for oxidising conditions when pH > 7.2 (Table 2, Figure 9) [5,8,38,86,88–90]:

$$ZnS + H^+ \rightleftharpoons HS^- + Zn^{+2} \quad (10)$$

$$Zn_5(OH)_6(CO_3)_2 + 8H^+ \rightleftharpoons 2HCO_3^- + 5Zn^{+2} + 6H_2O \quad (11)$$

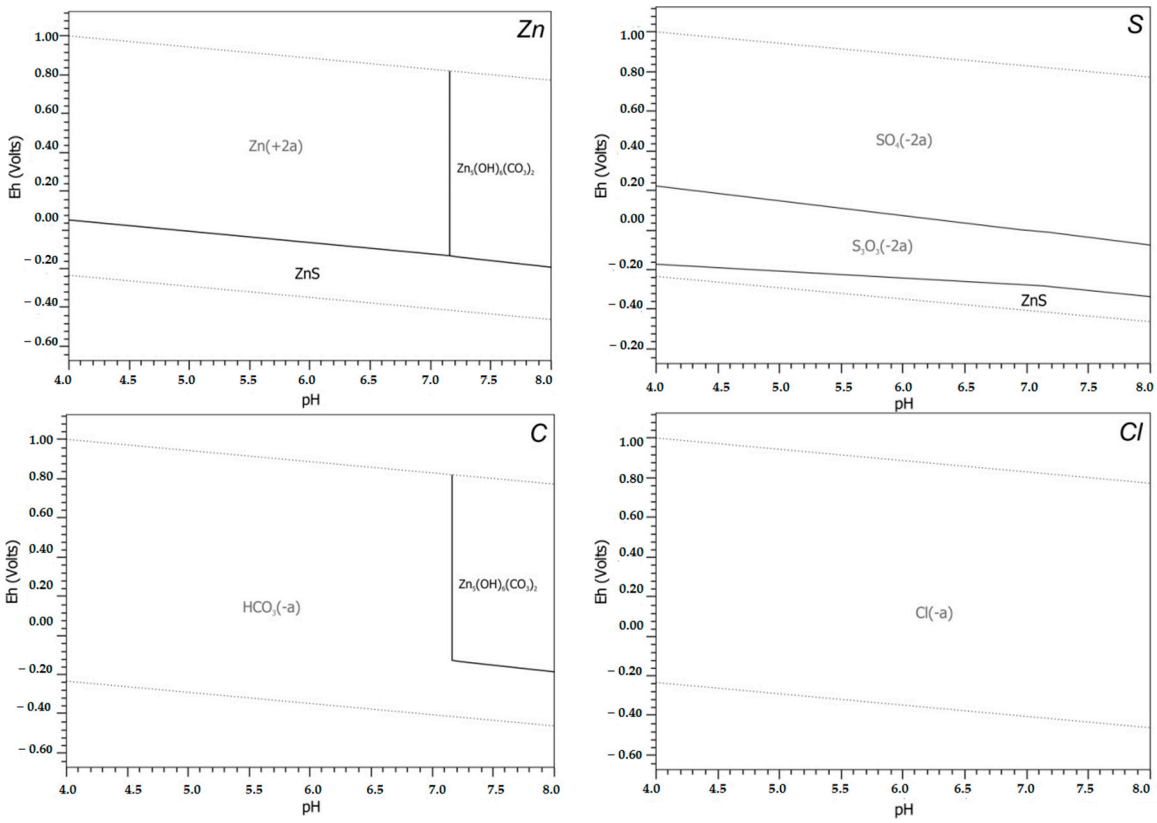

Figure 9. Eh-pH diagrams for ZnS, taking into account the presence of CO_2 and Cl ions in the environment (temperature T = 17 °C) [5].

Cd and As, released with ZnS into the environment, are present, as in the case of PbS, only in ionic forms, while Sb is present in the molecular forms SbO_2 and Sb_2O_3.

Analysis of the Eh-pH diagrams reveals an increase in the areas of $Sn(OH)_4$ and $SnSO_4$ stability regions at the expense of the corrosion regions, i.e., $Sn(OH)_3^+$ and $Sn(OH)_5^-$ mobility, compared to diagrams produced for $PbSO_4$ and PbS [39].

Willemite decomposes in the soil and water environment of the smelter plant, and the only form of zinc present in this environment is the mobile ionic form Zn^{2+} (Table 2, Figure 10). Willemite, despite belonging to the group of weathering-resistant minerals [5,38,90–100], is under hypergenic environment conditions a relatively mobile constituent of the landfilled refining slag (Equations (12)–(14)) [73,97]:

$$Zn_2SiO_4 + 4H+ \rightleftharpoons 2Zn^{2+} + H_4SiO_4 \quad (12)$$

$$H_4SiO_4 \rightleftharpoons SiO_2 + 2H_2O \quad (13)$$

$$H_2Si_2O_5 \rightleftharpoons 2SiO_2 + H_2O \quad (14)$$

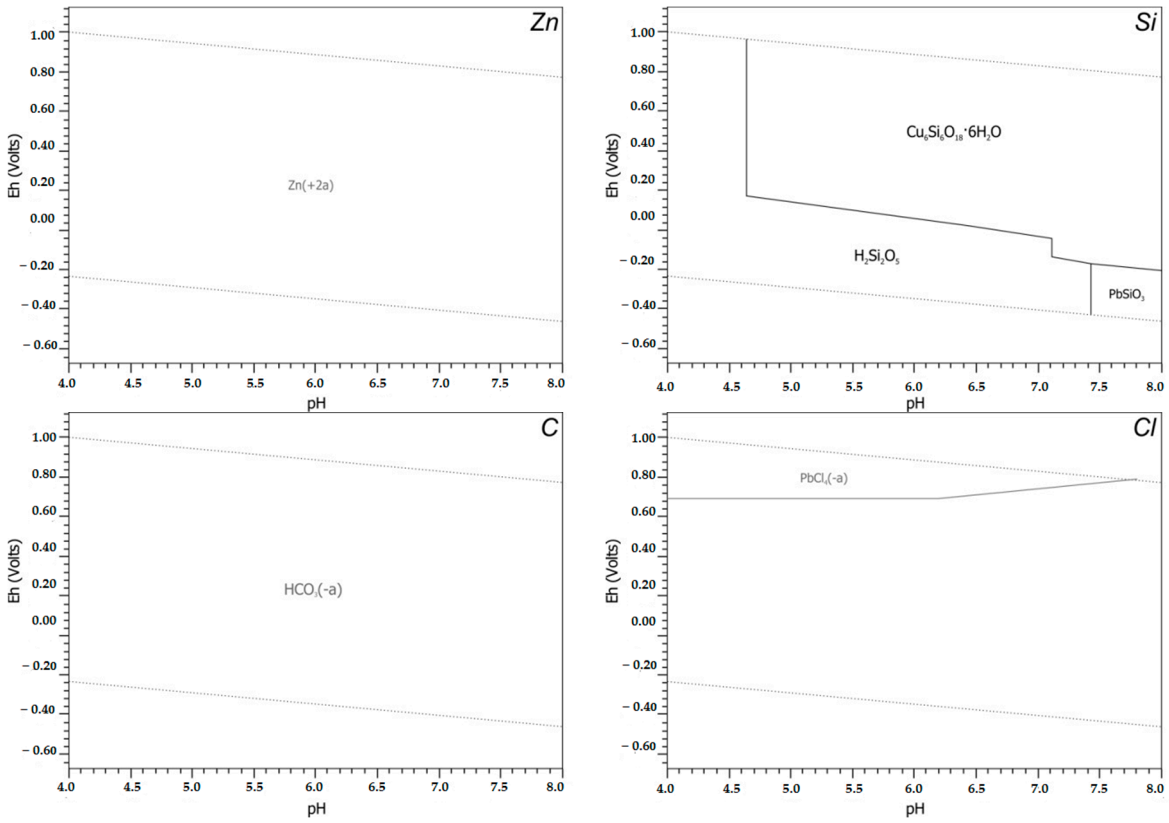

Figure 10. Eh-pH diagrams for Zn_2SiO_4, taking into account the presence of CO_2 and Cl ions in the environment (temperature T = 17 °C) [5].

The predominant forms of arsenic present with Zn_2SiO_4, which decomposes in the environment under study, are a variety of ions, where the only oxidation state of As is +5. The stable forms of As found under oxidising conditions within narrow pH ranges are mainly copper arsenates, less frequently hydrated arsenic oxides. [5,6,39,90–94,97–100].

The copper present in willemite in an oxidising environment is in the form of stable $Cu_6Si_6O_{18}·6H_2O$, while in weakly oxidising and reducing environments, the following forms are characteristic: stable $Cu(AsO_2)_2$ and mobile forms Cu^{2+} and $CuH_2AsO_3^+$.

In a hypergenic environment, the predominant forms of lead present in willemite are the following ions: Pb^{2+}, $PbCl_4^-$, and $PbOH^+$, while lead in the form of silicate $PbSiO_3$ occurs only in a narrow region of stability under reducing conditions in an alkaline environment [5,6,37,79,88,96–98].

Antimony, unlike $PbSO_4$, PbS, and ZnS, released from Zn_2SiO_4 into the environment, occurs there not only in a stable oxide form but also in a mobile ionic form characteristic of oxidising conditions at pH < 6.0 [5,6,39,98,99].

6. Summary and Conclusions

The most important factors that determine the mobility of elements released from refining slags include the following: the chemical and mineral composition of the waste and the environmental conditions.

Refining slags from Zn-Pb metallurgy have varied chemical and mineral compositions. The chemical composition of slags and the conditions of crystallisation of the phase constituents (temperature, cooling rate) determine their mineralogical composition. The phase

composition of slags is dominated by multiphase crystalline conglomerates formed with high-temperature processes. Typical mineral constituents in these slags include Zn and Fe oxides, Fe hydroxides, Zn, Pb, Fe and Cu sulphides, Pb sulphates, and hydrated Zn, Ca, Cu sulphates, Zn silicates, olivine group silicates, melilites $(Ca,Na)_2(Al,Mg)[(Si,Al)_2O_7]$, Pb and Zn carbonates, spinels, and multicomponent metal alloys of Pb, Zn, Cu, Fe, As, and Sb.

The most mobile constituents of the slags in the hypergenic environment studied are lead phases (anglesite and galena) and, to a lesser extent, zinc phases (sphalerite and willemite).

Anglesite and galena, together with dopant elements, decompose into ionic forms almost across the entire Eh-pH range. Sphalerite in the soil and water environment (oxidising and acidic conditions) decomposes into the mobile ionic form Zn^{2+}. The weathering-resistant willemite will undergo similar decomposition, but Zn^{2+} may be accompanied by silicate forms of the dopant elements (Cu and Pb) released from it. The dopant elements As and Cd released from the main phases into the environment occur mainly in mobile, toxic ionic forms, while Cu and Sb pose much less of a threat due to the stability of their forms of occurrence.

The bottom line is that slags from zinc and lead metallurgy, due to their chemical and phase composition, pose a potential threat to the environment, e.g., through the release of toxic elements into the environment.

Author Contributions: Conceptualization, K.N. and M.K.-P.; investigation, K.N.; resources, M.K.-P. and K.N.; data curation, M.K.-P.; writing—original draft preparation, K.N.; writing—review and editing, K.N. and M.K.-P.; visualization, M.K.-P.; supervision, K.N.; project administration, K.N. All authors have read and agreed to the published version of the manuscript.

Funding: This research received no external funding.

Conflicts of Interest: The authors declare no conflict of interest.

References

1. Piatak, N.M.; Ettler, V.; Hoppe, D. Geochemistry and Mineralogy of Slags. In *Metallurgical Slags: Environmental Geochemistry and Resource Potential*, 1st ed.; Piatak, N.M., Ettler, V., Eds.; Royal Society of Chemistry: London, UK, 2021.
2. Vítková, M. Environmental Characteristics of Mineral Waste from Metallurgy. Ph.D. Thesis, Charles University, Prague, Czech Republic, 2012.
3. Yin, N.H.; Lens, P.N.; Sivry, Y.; Hullebusch, E.D. Lead and Zinc Metallurgical Slags Mineralogy and Weathering. In *Sustainable Heavy Metal Remediation*; Springer: Berlin/Heidelberg, Germany, 2017; pp. 133–160. Available online: https://www.springer.com/series/11480 (accessed on 1 March 2024).
4. Piatak, N.M.; Parsons, M.B.; Seal, R.R., II. Characteristics and environmental aspects of slag: A review. *Applied Geochemistry* **2015**, *57*, 236–266. [CrossRef]
5. Nowińska, K. *Formy Występowania Metali w żużlach z Hutnictwa Cynku i ołowiu w Aspekcie Środowiskowym i Możliwości ich Odzysku*; Wydawnictwo Politechniki Śląskiej: Gliwice, Poland, 2022.
6. Ettler, V.; Vitková, M. Slag Leaching Properties and Release of Contaminants. In *Metallurgical Slags: Environmental Geochemistry and Resource Potential*, 1st ed.; Piatak, N.M., Ettler, V., Eds.; Royal Society of Chemistry: London, UK, 2021.
7. Piatak, N.M. *Environmental Characteristics and Utilization Potential of Metallurgical Slag*; Environmental Geochemistry; Elsevier: Amsterdam, The Netherlands, 2018; pp. 487–519. [CrossRef]
8. Adamczyk, Z.; Nowińska, K. Environmental mobility of trace elements present in dusts emitted from Zn-Pb metallurgical processes. *Environ. Earth Sci.* **2016**, *75*, 956. [CrossRef]
9. Nowińska, K.; Adamczyk, Z. Effect of galena contained in dust from Zn–Pb metallurgical processes on environment. *Environ. Earth Sci.* **2021**, *80*, 294. [CrossRef]
10. Babu, M.N.; Sahu, K.K.; Pandey, B.D. Zinc Recovery from Sphalerite Concentrate by Oxidative Leaching with Ammonium, Sodium and Potassium Persulphates. *Hydrometallurgy* **2002**, *64*, 119–129.
11. Santos, S.M.C.; Ismael, M.R.C.; Correia, M.J.N.; Reis, M.T.A.; Deep, A.; Carvalho, J.M.R. Hydrometallurgical Treatment of a Zinc Concentrate by Atmospheric Direct Leach Process. In Proceedings of the European Congress of Chemical Engineering (ECCE-6), Copenhagen, Denmark, 16–20 September 2007.
12. Filippou, D. Innovative hydrometallurgical processes for the primary processing of zinc. *Miner. Process. Extr. Rev.* **2004**, *25*, 205–252.
13. Sahu, K.; Agrawal, A. Lead, Zinc Extraction Processes. In Proceedings of the Extraction of Nonferrous Metals and Their Recycling—A Training Programme, Jamshedpur, India, 27–29 February 2008.

14. Sohn, H.Y.; Olivas-Martinez, M. Zinc and Lead Production. In *Treatise on Process Metallurgy*, 1st ed.; Seshadri Seetharaman; Elsevier: Amsterdam, The Netherlands, 2014; p. 671.
15. Hoang, J.; Reuter, M.; Matusewicz, R.; Hughes, S.; Piret, N. Top submerged lance direct zinc smelting. *Miner. Eng.* **2009**, *22*, 742–751. [CrossRef]
16. Chodkowski, S. *Metalurgia Metali Nieżelaznych*; Wydawnictwo Śląsk: Katowice, Poland, 1971.
17. Vignes, A. *Extractive Metallurgy 3*; Willey: Hoboken, NJ, USA, 2013.
18. Zhao, B. Lead and zinc sintering. In *Sintering Applications*; InTech: Rijeka, Croatia, 2013; pp. 165–199.
19. Matinde, E.; Steenkamp, J.D. Metallurgical Overview and Production of Slags. In *Metallurgical Slags: Environmental Geochemistry and Resource Potential*, 1st ed.; Piatak, N., Ettler, V., Eds.; Royal Society of Chemistry: London, UK, 2021.
20. Habashi, F. Retorts in the Production of Metals. A Historical Survey. *Metall* **2012**, *66*, 149–155.
21. Jędrychowska, S.; Wieczorek, A. Analiza wielopierwiastkowa środków smarowych z wykorzystaniem techniki spektrometrii fluorescencji rentgenowskiej z dyspersją fali. *Nafta-Gaz* **2013**, *6*, 476–485.
22. Tessadri, R. *Analytical Techniques for Elemental Analysis of Minerals*; Encyclopedia of Life Support Systems (EOLSS): Oxford, UK, 2009.
23. Bulska, E.; Wagner, B. Quantitative aspects of inductively coupled plasma mass spectrometry. *Philos. Trans. A Math. Phys. Eng. Sci.* **2016**, *347*, 20150369. [CrossRef]
24. Helaluddin, A.B.M.; Khalid, R.S.; Alaama, M.; Abbas, S.A. Main Analytical Techniques Used for Elemental Analysis in Various Matrices. *Trop. J. Pharm. Res.* **2016**, *15*, 427.
25. Will, G. *Powder Diffraction: The Rietveld Method and the Two Stage Method to Determine and Refine Crystal Structures from Powder Diffraction Data*; Springer: Berlin, Germany, 2006.
26. Llovet, X.; Moy, A.; Pinard, P.T.; Fournelle, J.H. Electron probe microanalysis: A review of recent developments and applications in materials science and engineering. *Prog. Mater. Sci.* **2021**, *116*, 100673. [CrossRef]
27. Fournier, C.; Merlet, C.; Dugne, O.; Fialin, N. Standardless semi-quantitative analysis with WDS-EPM. *J. Anal. At. Spectrom.* **1999**, *14*, 381–386. [CrossRef]
28. Bużantowicz, M.; Bużantowicz, W. Zastosowanie mikroskopii skaningowej do inspekcji układów elektronicznych wykonanych w technologii SMT. *Mechanik* **2013**, *7*, 71–76.
29. Kosson, D.S.; van der Sloot, H.A.; Sanchez, F.; Garrabrant, A.C. An integrated framework for evaluating leaching in waste management and utilization of secondary materials. *Environ. Eng. Sci.* **2002**, *19*, 159–204. [CrossRef]
30. Shanmuganathan, P.; Lakshmipathiraj, P.; Srikanth, S.; Nachiappan, A.L.; Sumathy, A. Toxicity characterization and long-term stability studies on copper slag from the ISASMELT process. *Resour. Conserv. Recycl.* **2008**, *52*, 601–611. [CrossRef]
31. *EN 12457-2:2002*; Characterisation of Waste—Leaching—Compliance Test for Leaching of Granular Waste Materials and Sludges—Part 2: One Stage Batch Test at a Liquid to Solid Ratio of 10 L/kg for Materials with Particle Size below 4 mm (without or with Size Reduction). European Committee for Standardisation: Brussels, Belgium, 2002.
32. *ASTM-D5284*; Standard Test Method for Sequential Batch Extraction of Waste with Acidic Extraction Fluid. ASTM International: West Conshohocken, PA, USA, 2009.
33. Cappuyns, V.; Alian, V.; Vassilieva, E.; Swennen, R. pH Dependent Leaching Behavior of Zn, Cd, Pb, Cu and As from Mining Wastes and Slags: Kinetics and Mineralogical Control. *Waste Biomass Valorizatio* **2014**, *5*, 355–368. [CrossRef]
34. Nang-Htay, Y.; Sivry, Y.; Guyot, F.; Lens, P.N.; van Hullebusch, E.D. Evaluation on chemical stability of lead blast furnace (LBF) and imperial smelting furnace (ISF) slags. *J. Environ. Manag.* **2016**, *180*, 310–323. [CrossRef]
35. Ganne, P.; Cappuyns, V.; Vervoort, A.; Buvé, L.; Swennen, R. Leachability of heavy metals and arsenic from slags of metal extraction industry at Angleur (eastern Belgium). *Sci. Total Environ.* **2006**, *356*, 69–85. [CrossRef]
36. Ettler, V.; Jehlička, J.; Mašek, V.; Hruška, J. The leaching behaviour of lead metallurgical slag in high-molecular-weight (HMW) organic solutions. *Mineral. Mag.* **2005**, *69*, 737–747. [CrossRef]
37. Parkhurst, D.L.; Appelo, C.A.J. Description of input and examples for PHREEQC version 3–A computer program for speciation, batch-reaction, one-dimensional transport, and inverse geochemical calculations. *US Geol. Surv. Tech. Methods* **2013**, *6*, 497.
38. Barna, R.; Bae, H.R.; Méhu, J.; Van der Sloot, H.; Moszkowicz, P.; Desnoyers, C. Assessment of Chemical Sensitivity of Waelz Slag. *Waste Manag.* **2000**, *20*, 115–124. [CrossRef]
39. Brookins, D.G. *Eh-pH Diagrams for Geochemistry*; Springer: Berlin/Heidelberg, Germany, 1998.
40. Parsons, M.B.; Bird, D.K.; Einaudi, M.T.; Alpers, C.N. Geochemical and mineralogical controls on trace element release from the Penn Mine base-metal slag dump, California. *Appl. Geochem.* **2001**, *16*, 1567–1573. [CrossRef]
41. Adamczyk, Z.; Melaniuk-Wolny, E.; Nowińska, K. *The Mineralogical and Chemical Study of Feedstock Mixtures and by-Products from Pyrometallurgical Process of Zinc and Lead Production*; Wydawnictwo Politechniki Śląskiej: Gliwice, Poland, 2010.
42. Piatak, N.M.; Seal, R.R.; Hammarstrom, J.M.; Meier, A.L.; Briggs, P.H. Geochemical Characterization of Slags, Other Mine Waste, and Their Leachate from the Elizabeth and Ely Mines (Vermont), the Ducktown Mining District (Tennessee), and the Clayton Smelter Site (Idaho). U.S. Department of the Interior, U.S. Geological Survey. 2003. Available online: https://pubs.usgs.gov/sir/2006/5303/ (accessed on 1 January 2024).
43. De Andrade Lima, L.R.P.; Bernardez, L.A. Characterization of the lead smelter slag in Santo Amaro, Bahia, Brazil. *J. Hazard. Mater.* **2011**, *189*, 692–699. [CrossRef] [PubMed]
44. Carpenter, J.S.; Bai, C.; Escobedo-Diaz, J.P.; Hwang, J.; Ikhmayies, S.; Li, B.; Li, J.; Sergio Monteiro, S.N.; Zhiwei, P.; Zhang, M. *Characterization of Minerals, Metals, and Materials*; Wiley: Hoboken, NJ, USA, 2015.

45. Kicińska, A. Physical and chemical characteristics of slag produced during Pb refining and the environmental risk associated with the storage of slag. *Environ. Geochem. Health* **2021**, *43*, 2723–2741. [CrossRef]
46. Harvey, W.; Downs-Rose, G. The Bay Mine, Wanlockhead, Scotland. *Br. Min.* **1976**, *2*, 1–9.
47. Ettler, V.; Legendre, O.; Bodénan, F.; Touray, J. Primary phases and natural weathering of old lead–zinc pyrometallurgical slag from Příbram, Czech Republic. *Can. Mineral.* **2001**, *39*, 873–888. [CrossRef]
48. Adamczyk, Z.; Nowińska, K. Phase composition of metallurgical zinc and lead slags. *Civ. Environ. Eng. Rep.* **2013**, *1*, 13–21.
49. Puziewicz, J.; Zainoun, K.; Bril, H. Primary phases in pyrometallurgical slags from a zinc-smelting waste dump, Świętochłowice, Upper Silesia, Poland. *Can. Mineral.* **2007**, *45*, 1189–1200. [CrossRef]
50. Bril, H.; Zainou, K.; Puziewicz, J.; Court In-Nomade, A.; Vanaecker, M.; Bollinger, J.-C. Secondary phases from the alteration of a pile of zinc-smelting slag as indicators of environmental conditions: An example from Świętochłowice, Upper Silesia, Poland. *Can. Mineral.* **2008**, *46*, 1235–1248. [CrossRef]
51. Ettler, V.; Johan, Z.; Kříbek, B.; Šebek, O.; Mihaljevic, M. Mineralogy and environmental stability of slags from the Tsumeb smelter, Namibia. *Appl. Geochem.* **2009**, *24*, 1–15. [CrossRef]
52. Kierczak, J.; Pietranik, A. Mineralogy and composition of historical Cu slags from the Rudawy Janowickie mountains, southwestern Poland. *Can. Mineral.* **2011**, *49*, 1281–1296. [CrossRef]
53. Sueoka, Y.; Sakakibara, M. Primary Phases and Natural Weathering of Smelting Slag at an Abandoned Mine Site in Southwest Japan. *Minerals* **2013**, *3*, 412–426. [CrossRef]
54. Warchulski, R.; Doniecki, T.; Gawęda, A.; Szopa, K. Composition and weathering of Zn-Pb slags from Bytom—Piekary Śląskie area: A case of heavy metal concentration and mobility. *Mineral.—Spec. Pap.* **2012**, *40*, 132–133.
55. Warchulski, R.; Doniecki, T.; Gawęda, A.; Szopa, K. Secondary phases from the Zn-Pb smelting slags from Katowice–Piekary Śląskie area, Upper Silesia, Poland: A SEM–XRD overview. *Mineral.—Spec. Pap.* **2014**, *42*, 110.
56. Warchulski, R.; Gawęda, A.; Janeczek, J.; Kędziołka-Gaweł, M. Mineralogy and origin of coarse-grained segregations in the pyrometallurgical Zn-Pb slags from Katowice-Wełnowiec (Poland). *Mineral. Petrol.* **2016**, *110*, 681–692. [CrossRef]
57. Warchulski, R.; Gawęda, A.; Kądziołka-Gaweł, M.; Szopa, K. Composition and element mobilization in pyrometallurgical slags from the Orzeł Biały smelting plant in the Bytom-Piekary Śląskie area, Poland. *Mineral. Mag.* **2015**, *79*, 459–483. [CrossRef]
58. Potysz, A. Copper Metallurgical Slags: Mineralogy, Bioweathering Processes and Metal Bioleaching. Ph.D. Thesis, Universit'e Paris-Est, Paris, France, 2015.
59. Nowińska, K. Mineralogical and chemical characteristics of slags from the pyrometallurgical extraction of zinc and lead. *Minerals* **2020**, *10*, 371. [CrossRef]
60. Nowińska, K.; Adamczyk, Z. Slags of the imperial smelting process for Zn and Pb production. In *Reference Module in Materials Science and Materials Engineering*; Saleem, H., Ed.; Elsevier: Amsterdam, The Netherlands, 2017; pp. 1–5. [CrossRef]
61. Mendecki, M.; Warchulski, R.; Szczuka, M.; Środek, D.; Pierwoła, J. Geophysical and petrological studies of the former lead smelting waste dump in Sławków, Poland. *J. Appl. Geophys.* **2020**, *179*, 104080. [CrossRef]
62. Ettler, V.; Kierczak, J. Environmental Impact of Slag Particulates. In *Metallurgical Slags: Environmental Geochemistry and Resource Potential*, 1st ed.; Piatak, N.M., Ettler, V., Eds.; Royal Society of Chemistry: London, UK, 2021.
63. Warr, L.N. IMA–CNMNC approved mineral symbols. *Mineral. Mag.* **2021**, *85*, 291–320. [CrossRef]
64. Ettler, V.; Johan, Z.; Touray, J.C.; Jelínek, E. Zinc partitioning between glass and silicate phases in historical and modern lead–zinc metallurgical slags from the Příbram district, Czech Republic. *Earth Planet. Sci.* **2000**, *331*, 245–250. [CrossRef]
65. Ettler, V. Etude du Potential Pollutant de Rejets Anciens et Actuels de la Métallurgie du Plomb Dans le district de Příbram (République tchèque). Ph.D. Thesis, Université d'Orléans, France and Charles University, Prague, Czech Republic, 2000.
66. Ettler, V.; Piantone, P.; Touray, J.C. Mineralogical control on inorganic contaminant mobility in leachate from lead-zinc metallurgical slag: Experimental approach and long-term assessment. *Mineral. Mag.* **2003**, *67*, 1269–1283. [CrossRef]
67. Ettler, V.; Johan, Z. 12 years of leaching of contaminants from Pb smelter slags: Geochemical/mineralogical controls and slag recycling potential. *Appl. Geochem.* **2014**, *40*, 97–103. [CrossRef]
68. Ettler, V.; Komarkova, M.; Jechlicka, J.; Coufal, P.; Hradil, D.; Machovic, V.; Delorme, F. Leaching of lead metallurgical slag in citric solutions—Implications for disposal and weathering in soil environments. *Chemosphere* **2004**, *57*, 167–177. [CrossRef]
69. Ettler, V.; Vaněk, A.; Mihaljevič, M.; Bezdička, P. Contrasting lead speciation in forest and tilled soils heavily polluted by lead metallurgy. *Chemosphere* **2005**, *58*, 1449–1459. [CrossRef]
70. Mizerna, K.; Król, A. Wpływ wybranych czynników na wymywalność metali ciężkich z odpadu hutniczego. *Inżynieria Ekol.* **2015**, *43*, 1–6. [CrossRef] [PubMed]
71. Seignez, N.; Gauthier, A.; Bulteel, D.; Damidot, D.; Potdevina, J.L. Leaching of lead metallurgical slags and pollutant mobility far from equilibrium conditions. *Appl. Geochem.* **2008**, *23*, 3699–3711. [CrossRef]
72. Potysz, A.; Kierczak, J.; Pietranik, A.; Kadziolka, K. Mineralogical, geochemical, and leaching study of historical Cu-slags issued from processing of the Zechstein formation (Old Copper Basin, southwestern Poland). *Appl. Geochem.* **2018**, *98*, 22–35. [CrossRef]
73. Ettler, V.; Kvapil, J.; Šebek, O.; Johan, Z.; Mihaljevič, M.; Ratié, G.; Garnier, J.; Quantin, C. Leaching behaviour of slag and fly ash from laterite nickel ore smelting (Niquelândia, Brazil). *Appl. Geochem.* **2016**, *64*, 118–127. [CrossRef]
74. Vitkova, M.; Ettler, V.; Mihaljevic, M.; Sebek, O. Effect of sample preparation on contaminant leaching from copper smelting slag. *J. Hazard. Mater.* **2011**, *197*, 417–423. [CrossRef]

75. Saikia, N.; Cornelis, G.; Mertens, G.; Elsen, J.; Van Balen, K.; Van Gerven, T.; Vandecasteele, C. Assessment of Pb-slag, MSWI bottom ash and boiler and fly ash for using as a fine aggregate in cement mortar. *J. Hazard. Mater.* **2008**, *154*, 766–777. [CrossRef]
76. Saikia, N.; Cornelis, G.; Cizer, Ö.; Vandecasteele, C.; Van Gemert, D.; Van Balen, K.; Van Gerven, T. Use of Pb blast furnace slag as a partial substitute for fine aggregate in cement mortar. *J. Mater. Cycles Waste Manag.* **2012**, *14*, 102–112. [CrossRef]
77. Jarošíková, A.; Ettler, V.; Mihaljevič, M.; Kříbek, B.; Mapani, B. The pH-dependent leaching behavior of slags from various stages of a copper smelting process: Environmental implications. *J. Environ. Manag.* **2017**, *187*, 178–186. [CrossRef]
78. Potysz, A.; Kierczak, J.; Fuchs, Y.; Grybos, M.; Guibaud, G.; Lens, P.N.L.; van Hullebusch, E.D. Characterization and pH-dependent leaching behaviour of historical and modern copper slags. *J. Geochem. Explor.* **2016**, *160*, 1–15. [CrossRef]
79. Mizerna, K. Mobility of heavy metals from metallurgical waste in the context of sustainable waste management. *Econ. Environ. Stud.* **2016**, *16*, 819–830.
80. Štulović, M.; Ivšić-Bajčeta, D.; Ristić, M.; Kamberović, Ž.; Korać, M.; Anđić, Z. Leaching properties of secondary lead slag stabilized/solidified with cement and selected additives. *Environ. Prot. Eng.* **2013**, *39*, 149–163. [CrossRef]
81. Scheetz, C.D.; Rimstidt, J.D. Dissolution, transport, and fate of lead on a shooting range in the Jefferson National Forest near Blacksburg, VA, USA. *Environ. Geol.* **2009**, *58*, 655–665. [CrossRef]
82. Song, Y.; Wilson, M.J.; Moon, H.S.; Bacon, J.R.; Bain, D.C. Chemical and mineralogical forms of lead, zinc and cadmium in particle size fractions of some wastes, sediments and soils in Korea. *Appl. Geochem.* **1999**, *14*, 621–633. [CrossRef]
83. Taylor, P.; Lopata, V.J. Stability and solubility relationships between some solids in the system PbO-CO_2-H_2O. *Can. J. Chem.* **1983**, *62*, 395–402. [CrossRef]
84. Jolley, L.R.; Campenter, J.H. *Aqueous Chemistry of Chlorine; Chemistry, Analysis, and Environmental Fate of Reactive Oxidant Species*; Oak Ridge National Laboratory: Oak Ridge, TN, USA, 1982.
85. Uhler, A.D.; Helz, G.R. Solubility product of galena at 298°K: A possible explanation for apparent supersaturation in nature. *Geochim. Et Cosmochim. Acta* **1984**, *48*, 1155–1160. [CrossRef]
86. Kushnir, C.S.E. Influence of Water Chemistry Parameters on the Dissolution Rate of the Lead (II) Carbonate Hydrocerussite. Master's Thesis, The University of Western Ontario, London, ON, Canada, 2014.
87. Mohammadzadeh, M.; Basu, O.D.; Herrera, J.E. Impact of water chemistry on lead carbonate dissolution in drinking water distribution systems. *J. Water Resour. Prot.* **2015**, *7*, 389–397. [CrossRef]
88. Ray, P.; Datta, S.P. Solid phase speciation of Zn and Cd in zinc smelter effluent-irrigated soils. *Chem. Speciat. Bioavailab.* **2017**, *29*, 6–14. [CrossRef]
89. Nordstrom, K.; Majzlan, J.; Königsberger, E. Thermodynamic properties for arsenic minerals and aqueous species. *Rev. Mineral. Geochem.* **2014**, *79*, 217–254. [CrossRef]
90. Štulović, M.; Radovanović, D.; Kamberović, Ž.; Korać, M.; Anđić, Z. Assessment of Leaching Characteristics of Solidified Products Containing Secondary Alkaline Lead Slag. *Int. J. Environ. Res. Public Health* **2019**, *16*, 2005. [CrossRef]
91. Brugger, J.; Mcphail, D.C.; Wallace, M.; Waters, J. Formation of willemite in hydrothermal environments. *Econ. Geol.* **2003**, *98*, 819–835. [CrossRef]
92. Najera Ibarra, J.M.; Soria-Aguilar, M.J.; Martínez-Luevanos, A.; Picazo-Rodriguez, N.G.; Almaguer-Guzman, I.; Chaidez-Felix, J.; Carrillo-Pedroza, S.F.R. Zinc Extraction from Primary Lead Smelting Slags by Oxidant Alkaline Leaching. *Metals* **2024**, *12*, 1409. [CrossRef]
93. Kamberović, Ž.; Ranitović, M.; Korać, M.; Djokić, J.; Jevtić, S. Hydrometallurgical Process for Selective Metals Recovery from Waste-Printed Circuit Boards. *Metals* **2018**, *8*, 441. [CrossRef]
94. Vanaeckera, M.; Courtin-Nomadea, A.; Brila, H.; Laureyns, J.; Lenain, J.F. Behavior of Zn-bearing phases in base metal slag from France and Poland: A mineralogical approach for environmental purposes. *J. Geochem. Explor.* **2014**, *136*, 1–14. [CrossRef]
95. Ford, R.G.; Wilkin, R.T. *Monitored Natural Attenuation of Inorganic Contaminants in Ground Water Volume 2—Assessment for Non-Radionuclides Including Arsenic, Cadmium, Chromium, Copper, Lead, Nickel, Nitrate, Perchlorate, and Selenium*; Report number: EPA/600/R-07/140; U.S. Environmental Protection Agency: Washington, DC, USA, 2007.
96. Missimer, T.M.; Teaf, C.M.; Beeson, W.T.; Maliva, R.G.; Woolschlager, J.; Covert, D.J. Natural background and anthropogenic arsenic enrichment in Florida soils, surface water and groundwater: A Review with a Discussion on Public Health Risk. *Int. J. Environ. Res. Public Health* **2018**, *15*, 2278. [CrossRef]
97. Potysz, A.; Kierczak, J.; Grybos, M.; Pędziwiatr, A. Weathering of historical copper slags in dynamic experimental system with rhizosphere-like organic acids. *J. Environ. Manag.* **2018**, *222*, 325–337. [CrossRef]
98. Potysz, A.; Hullebusch, E.D.; Kierczak, J.; Grybos, M.; Lens, P.N.; Guibaud, G. Copper Metallurgical Slags—Current Knowledge and Fate: A Review. *Crit. Rev. Environ. Sci. Technol.* **2015**, *45*, 2424–2488. [CrossRef]
99. Kucha, H.; Martens, A.; Ottenburgs, R.; De Vos, W.; Viaene, W. Primary minerals of Zn-Pb mining and metallurgical dumps and their environment behavior at Plombieres, Belgium. *Environ. Geol.* **1996**, *27*, 1–7. [CrossRef]
100. Navarro, A.; Cardellach, E.; Mendoza, J.L.; Corbella, M.; Domenech, L.M. Metal mobilization from base-metal smelting slag dumps in Sierra Almagrera (Almería, Spain). *Appl. Geochem.* **2008**, *23*, 895–913. [CrossRef]